ACES Asian Chemical Editorial Society

DOI: 10.1002/asia.201801676

CHEMISTRY AN ASIAN JOURNAL Communication

SPECIAL ISSUE

A Photostable AIEgen for Specific and Real-time Monitoring of Lysosomal Processes

Weijie Zhang[+],[a, b, d] Fan Zhou[+],[c] Zhiming Wang,*[a, c] Zujin Zhao,[c] Anjun Qin,[c] and Ben Zhong Tang*[a, c, d]

Abstract: Lysosomes are recognized as advanced organelles involved in many cellular processes and are also considered as crucial regulators of cell homeostasis. The current strategies for monitoring activities of lysosomes exhibit some limitations. Herein, we synthesized a novel fluorescent probe named 2M-DPAS with AIE characteristics, which was proved to have significant advantages of good biocompatibility, high selectivity, bright emission and excellent photostability. Based on those, 2M-DPAS can be used to continuously monitor the dynamic changes of lysosomes, including autophagy and mitophagy, as well as to track the process of endocytosis of macromolecules in lysosomes, which are of benefit to better know about the lysosomes-related diseases.

Lysosomes are the main digestive organelles in almost all eukaryotic cells and were first discovered by Christian de Duve in the 1950s.[1] They are contained by a single phospholipid-bilayer of 7–10 nm in which more than 25 membrane proteins have been identified.[2] The lumen of lysosomes contains more than 50 acid hydrolases, which are readily attached to alkaline substances.[3] The basic function of lysosomes is to digest extracellular macromolecules that have been internalized by endocytosis and intracellular metabolic organelles such as mitochondria that have been sequestered by autophagy.[4] To achieve these functions, lysosomes are continuously changing their morphology and spatial distribution, with their shapes ranging from spherical to tubular. Therefore, lysosomal disturbance has profound effects on cell homeostasis. Recently, it has been found that the positioning of lysosomes could be precisely controlled to meet the changing cellular needs. For example, under nutrient deprivation conditions, lysosomes could be rapidly recruited to the perinuclear region. Importantly, lysosomal dysfunction causes many diseases, such as cancer and Alzheimer's disease.[5] In view of the essential functions of lysosomes, imaging and monitoring the dynamic changes of lysosomal morphology and spatial distribution are highly useful in the management of lysosomal related diseases.

The most common strategies used to visualize and monitor lysosomes apply compounds whose pH-dependent fluorescence is weak in basic and neutral conditions but can be "turned on" in acidic environments, such as the LysoSensor™ pH Indicator used as a commercial dye.[6] Other examples of labeling lysosomes include neutral red,[7] acridine orange,[8] LysoTracker,[9] dextran labeled with a fluorophore[10] and nanoparticles.[11,6c] Although these probes track the lysosomes effectively, they suffer many limitations. For example, the low specificity of neutral red and acridine orange for lysosomes, rapid photobleaching of LysoTracker,[9] and high cytotoxicity of nanoparticles and dextran,[10] limit their applications considerably. It is thus imperative to develop a new probe to image lysosomes with high specificity, good biocompatibility, excellent photostability and a high signal-to-noise ratio.

A novel photophysical phenomenon of aggregation-induced emission (AIE) was developed in our group since 2001.[12] Fluorogens with AIE (AIEgens) properties are highly emissive in the aggregation state but demonstrate faint emission in dilute solution, which is ideal for imaging and biosensing because of most organic emitters based on conjugated aromatic structure suffered from aggregation-caused quenching effect.[13] Restricted intramolecular motion (RIM) of AIEgens in the aggregation state was the main mechanism of the AIE effect by lots of experiments and calculation. So, many AIEgens were developed via utilizing this nature to image intramolecular organelles, but few of them were used to track and monitor lysosomes with their physiological processes.[14]

We have previously reported on lipid droplets-targeting DPAS (2-(((diphenylmethylene)hydrazono)-methyl)-phenol), which has excellent biocompatibility and monitoring dynamics.[15] In this work, we designed and synthesized a novel AIE fluorogen, namely 2M-DPAS, based on DPAS (Figure 1 A), and

[a] Dr. W. Zhang,[+] Dr. Z. Wang, Prof. B. Z. Tang
HKUST-Shenzhen Research Institute
Nanshan, Shenzhen, 518057 (China)
E-mail: wangzhiming@scut.edu.cn
tangbenz@ust.hk

[b] Dr. W. Zhang[+]
Urinary surgery, Affiliated first hospital
Soochow University
Pinghai Road, Suzhou, 215006 (China)

[c] F. Zhou,[+] Dr. Z. Wang, Prof. Z. Zhao, Prof. A. Qin, Prof. B. Z. Tang
State Key Laboratory of Luminescent Materials and Devices, Centre for Aggregation-Induced Emission,
South China University of Technology
Wushan Road, Guangzhou, 510640 (China)

[d] Dr. W. Zhang,[+] Prof. B. Z. Tang
Department of Chemistry and Department of Chemical and Biological Engineering
The Hong Kong University of Science and Technology
Clear Water Bay, Kowloon, Hong Kong (China)

[+] These authors have contributed equally to this work

Supporting information and the ORCID identification number(s) for the author(s) of this article can be found under: https://doi.org/10.1002/asia.201801676.

This manuscript is part of a special issue on π-Conjugated Compounds for Molecular Materials. Click here to see the Table of Contents of the special issue.

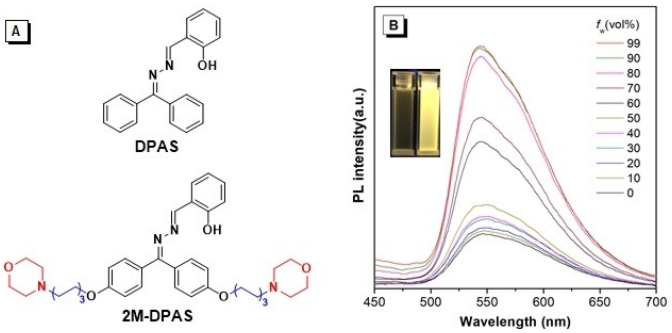

Figure 1. (A) The chemical structure of DPAS and 2M-DPAS. (B) PL spectra of 2M-DPAS in THF/water mixtures with different water fractions. [2M-DPAS] = 10 μM. (Inset: fluorescent images at f_w = 0% and f_w ≈ 99%).

its synthetic route and analysis data are shown in Scheme S1 and Figure S1, S2. The chain length of six carbons ensure probe flexibility and the two basic morpholine groups allow 2M-DPAS to easily target lysosomes which contain many acid hydrolases. As discussed further below, in our investigation of the potential of 2M-DPAS in monitoring the dynamic changes of lysosomes with autophagy, mitophagy and phagocytosis of macromolecules, 2M-DPAS consistently showed excellent performance.

The photophysical properties of 2M-DPAS were studied first. The absorption band of 2M-DPAS peaked at 415 nm in THF solution (Figure S3) while its emission peak location was observed at 550 nm (Figure 1 B). Thanks for its classical ESIPT emission process, the Stokes-shift of 2M-DPAS reaches to 135 nm, which is benefit to high quality imaging. In fact, 2M-DPAS emitted faintly in pure THF solutions, and its emission remained low even the solution contained a large amount of water (50 vol%). However, with further increase of the water fraction, 2M-DPAS fluoresced more strongly at 550 nm with a light-yellow color, a clear property of AIE, thus avoiding the ACQ problem with most of the conventional fluorescent probes of lysosomes. Obviously, the weak emission of 2M-DPAS in pure THF solutions was due to non-radiative decay caused by dynamic intramolecular motion, while in the aggregated state, the ESIPT process was activated and the strong emission from keto-form was shown due to the restricted intramolecular hydrogen bond motion.

With DPAS specifically targeting lipid droplets, the specificity of 2M-DPAS in cells was explored as well. We speculated that the basicity of the two morpholine groups would enable 2M-DPAS to accumulate in the acidic environments of lysosomes (pH 4.5–5.0). Thus, the well-known commercial lysosome-targeting dye Lysotracker Red (LTR) was co-stained with 2M-DPAS. As shown in Figure 2, green fluorescence from 2M-DPAS and red fluorescence from LTR are clearly visualized, respectively. The merged image shows that the distribution of 2M-DPAS in cells is totally consistent with that of LTR (Figure 2 D). The Pearson's correlation coefficient, which describes the degree of linear dependence between two variables, is 0.96, suggesting that 2M-DPAS specifically targets lysosomes. Additionally, 2M-DPAS showed a higher contrast than LTR under the same incubation time, which can be attributed to the

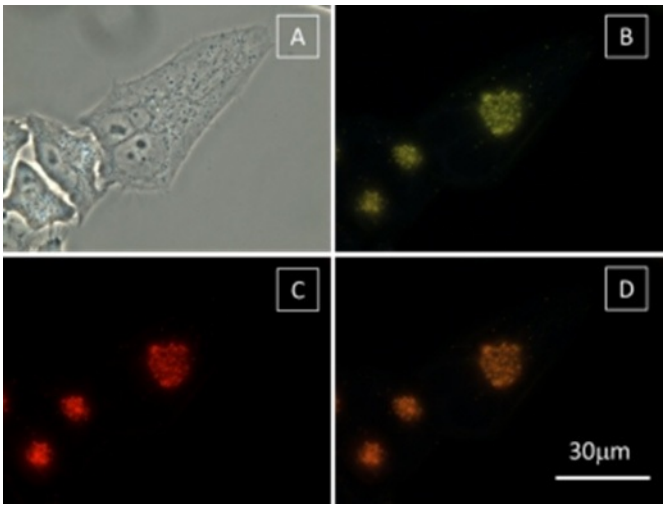

Figure 2. (A) Bright field and (B) fluorescent images of HeLa cells stained with 2M-DPAS (10 μM, 30 min) or (C) Lysotracker Red (75 nm, 30 min). (D) A superimposed image from (B) and (C). Scale bar = 30 μm.

bright emission and high selectivity of 2M-DPAS. Furthermore, the PL intensity of 2M-DPAS was tested in different pH buffered solutions. Besides, there was not a larger shift in emission peak location in aqueous solution and in lysosomes of Hela cells, implying its pH-independent properties (Figure S4).

Besides selectivity, photostability is considered one of the key factors in evaluating the performance of fluorescent imaging probes. The photostability of HeLa cells co-stained with 2M-DPAS and LTR was investigated by monitoring the fluorescence intensity before and after 30 consecutive scans by a confocal microscopy. As shown in Figure 3 A, the signal loss of 2M-

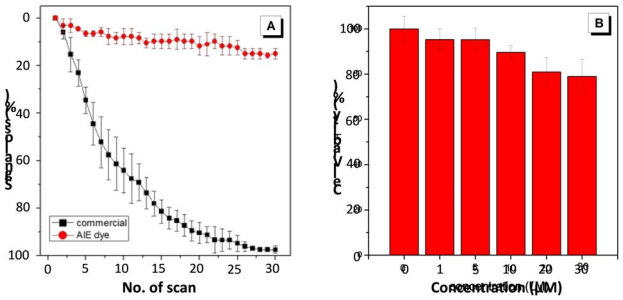

Figure 3. (A) Signal loss (%) of fluorescent emission of 2M-DPAS (red circles) and LTR (black squares) with increasing number of scans. (B) Cell viability of 2M-DABS evaluated on HeLa cells by MTT assay.

DPAS was less than 15% of the original intensity after 30 scans. In contrast, the fluorescence signal loss of LTR reached up to 95%. There were no significant differences observed between the first and the 30th fluorescence images of 2M-DPAS, whereas no fluorescence was observed in the 30th fluorescence image of LTR (Figure S5). The main reason was the difference in working concentrations of different fluorescent probes for lysosomal imaging due to their own properties. Truly, the working concentration of 2M-DPAS is up to 133 times that of LTR, resulting in higher brightness and photostability of 2M-

DPAS in lysosomal imaging. If the LTR reached this concentration, the fluorescence intensity would decrease greatly because its ACQ effect was activated. Thanks for the AIE nature of 2M-DPAS, the excellent photostability was realized, and the long-term lysosomal imaging could become possible.

In addition, the cytotoxicity of 2M-DPAS on HeLa cells was assessed using MTT assay to confirm the safety of 2M-DPAS in visualizing lysosomes. As illustrated in Figure 3B, when the cells were incubated with up to 20 mM of 2M-DPAS for 24 h, the cell viability remained above 80%. Even at concentration as high as 30 mM, the cell growth was not greatly impaired, indicating a weak effect of 2M-DPAS on cell growth. The excellent biocompatibility and photostability of 2M-DPAS therefore renders it a useful fluorescent probe for dynamically monitoring lysosomes during different physiological processes.

Autophagy is a process that transports damaged cells, degenerated or aging proteins, and organelles to the lysosomes for digestion and degradation. Visualizing and tracking activities of lysosomes enrich the insight into the process of autophagy given the close association of lysosomes and autophagy. Considering that 2M-DPAS has high specificity for lysosomes and strong photostability, the ability of real-time monitoring of dynamic changes of autophagy was tested. Since mammalian target of rapamycin (mTOR) is an important suppressor of autophagy functioning upstream of the autophagy protein,[16] inhibition of mTOR potently up-regulates autophagy during the cellular response to the specific mTOR inhibitor, rapamycin.[17] As shown in Figure 4D–F, the lysosomes of HeLa cells can be

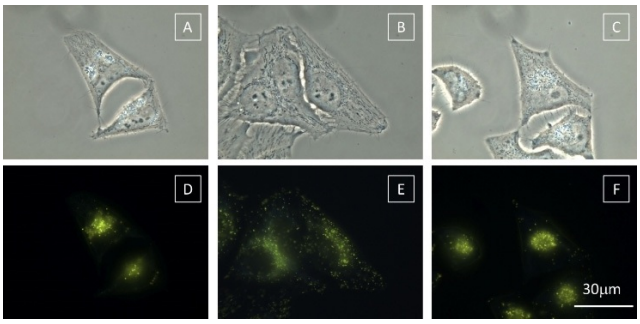

Figure 4. (A–C) Bright field and (D–F) fluorescent images of HeLa cells stained with 10 μM 2M-DPAS: (A, D) before treatment, (B, E) after treatment of rapamycin and (C, F) after treatment of rapamycin and 3-MA. Scale bar = 30 μm.

clearly visualized, with each green spot representing a lysosome under the fluorescence microscope. First, we found that the lysosomes increased in quantity and were widely distributed intracellularly after HeLa cells were treated with rapamycin (50 μg mL^{-1}), suggesting that the process of autophagy was monitored in real time (Figure 4E). Meanwhile, we also used 3-MA, a well characterized inhibitor of the early stage of autophagy.[18] As illustrated in Figure 4F, no obvious changes were observed in the quantity and spatial distribution of lysosomes 30 min after simultaneously adding 3-MA (10 mM) and rapamycin (50 μg mL^{-1}) into the culture medium of 2M-DPAS stained HeLa cells. This resulted from the addition of 3-MA to the HeLa cells, inhibiting the initial stage of autophagy despite the presence of rapamycin. Therefore, 2M-DPAS can accurately monitor the process of autophagy in real time, which, along with its high selectivity for lysosomes and excellent photostability, make it an excellent choice for investigating the process of autophagy.

Autophagy is a non-selective process whereby mitochondria are the targets of autophagy. Therefore, mitophagy can also be triggered by rapamycin.[19] As shown in Figure 5, different

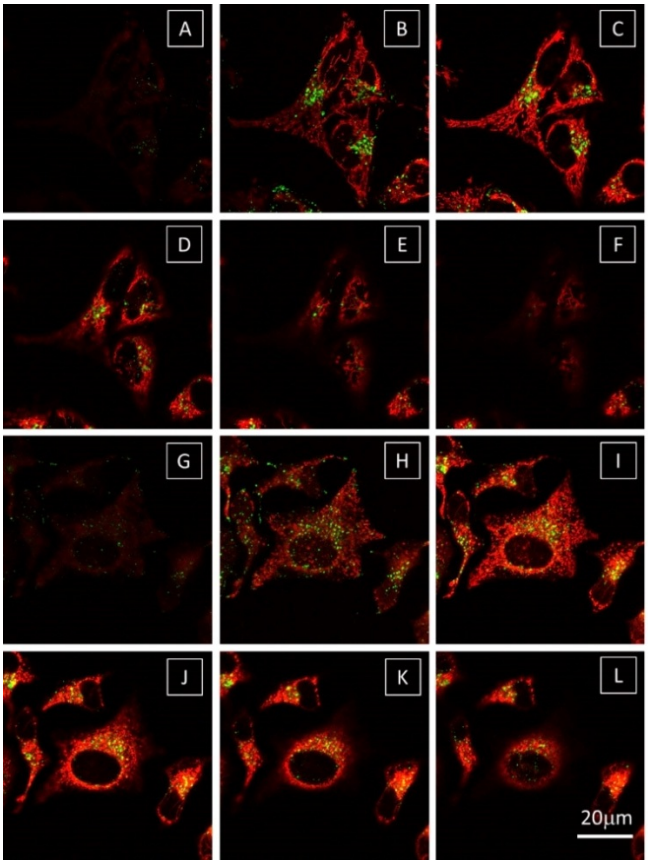

Figure 5. Fluorescent images of HeLa cells at different layers stained with 10 μM 2M-DPAS and 50 nM MTR (A–F) before treatment of rapamycin; Fluorescent images of HeLa cells at different layers stained with 10 μM 2M-DPAS and 50 nM MTR (G–L) after treatment of rapamycin. Scale bar = 20 μm.

layers of mitochondria could be clearly captured by confocal microscopy in HeLa cells co-stained with 2M-DPAS and Mito-Tracker Red (MTR) after treatment without or with rapamycin. The long filamentous structures of mitochondria were clearly shown in red from MTR while the punctate structures of lysosomes were well portrayed as green spots from 2M-DPAS. Compared with Hela cells cultured without rapamycin (Figure 5A–F) and with rapamycin (Figure 5G–L) (50 μg mL^{-1}) to induce mitophagy, pronounced changes had taken place in the quantity and spatial distribution of lysosomes and the morphology of mitochondria (Figure 5). The network structures of mitochondria appeared broken and punctate, and numerous lysosomes could be seen distributed widely in the three-dimensional layer of one mitochondrion. In addition, the coinci-

dence degree between lysosomes and mitochondria increased markedly. Therefore, the process of mitophagy was effectively monitored in the presence of 2M-DPAS and MTR, further demonstrating the superiority of 2M-DPAS in monitoring the dynamics of lysosomes.

Apart from digesting metabolic organelles such as mitochondria that have been sequestered by autophagy, lysosomes also serve to digest extracellular macromolecules that have been internalized by endocytosis. We have demonstrated that 2M-DPAS can monitor the process of autophagy and mitophagy, but can 2M-DPAS monitor the process of digesting extracellular macromolecules in the lysosomes? One of the pathological hallmarks of Alzheimer's disease (AD) is the formation of senile plaques composed primarily of aggregated amyloid β peptides (Aβ) in the brain. The Aβ aggregation is widely considered to have a causal role in the development of AD.[18] Therefore, the ability of 2M-DPAS to monitor lysosomal phagocytosis of macromolecules was tested using HMCs (human meningeal cells) and FAM-Aβ (FAM-labelled Aβ). As shown in Figure 6 (A–C, G–I), 1 h following FAM-Aβ treatment, there was no overlap between the green light emitted by FAM-Aβ and the red light from lysosomes labeled with 2M-DPAS or LTR, indicating that the passage of FAM-Aβ into lysosomes via endocytosis had not occurred. However, in Figure 6 D–F, J–L, 24 h after HMCs were treated with FAM-Aβ, several yellow spots were observed where lysosomes were labeled with 2M-DPAS or LTR, suggesting that FAM-Aβ had been phagocytosed by lysosomes labeled with 2M-DPAS or LTR. Therefore, 2M-DPAS can also monitor the lysosomal phagocytosis of macromolecules, while showing an advantage over LTR which requires a long time of laser irradiation. 2M-DPAS may be used to study the lysosomal processes in AD given the phagocytotic role of lysosomes in AD.

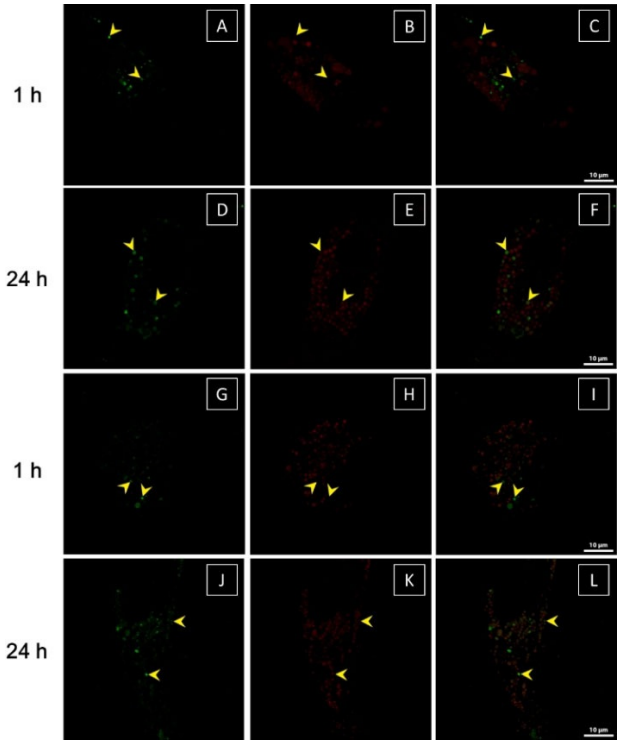

Figure 6. Fluorescent images of HMCs after treatment of 2 μM FAM-Aβ for 1 h (A) or 24 h (D), followed by 10 μM 2M-DPAS for 30 min (B, E). Merged fluorescent images of HMCs treatment and 2M-DPAS (C, F); Fluorescent images of HMCs after treatment of 2 μM FAM-Aβ for 1 h (G) or 24 h (J), followed by 50 nM LTR for 30 min (H, K) Merged fluorescent images of HMCs treatment and LTR (I, L). The yellow arrows indicate the locations of FAM-Aβ. Scale bar = 10 μm.

In summary, we have reported a novel fluorescent probe 2M-DPAS with AIE characteristics for specific lysosomal imaging. Its good biocompatibility, high selectivity, bright emission, pH-independence and excellent photostability enable continuous monitoring of the dynamic changes of lysosomes in real time. This probe has been demonstrated to effectively monitor and track the processes of autophagy, mitophagy and phagocytosis of macromolecules in lysosomes in real time. Importantly, 2M-DPAS could be a promising tool in the study of lysosome-related processes in Alzheimer's disease.

Acknowledgements

This work is financially supported by National Natural Science Foundation of China (21788102, 51673118, 81472401 and 51603127), Science & Technology Program of Guangzhou (201804010218), Science and Technology Plan of Shenzhen (JCYJ20160428150429072 and JCYJ20160229205601482), the Innovation and Technology Commission of Hong Kong (ITC-CNERC14S01), and the Fundamental Research Funds for the Central Universities (2015ZY013, 2017JQ013 and 2017B0036).

Conflict of interest

The authors declare no conflict of interest.

Keywords: aggregation-induced emission · autophagy · lysosomes · monitoring · phagocytosis of macromolecules

[1] a) F. Appelmans, R. Wattiaux, C. De Duve, *Biochem. J.* **1955**, *59*, 438–447; b) C. de Duve, *Amer. Physiol. Soc.* **1959**, 128.
[2] P. Saftig, B. Schroder, J. Blanz, *Biochem. Soc. Trans.* **2010**, *38*, 1420–1423.
[3] T. Lübke, P. Lobel, D. E. Sleat, *Biochimica et Biophysica (BBA)-Mol Cell Res.* **2009**, *1793*, 625–635.
[4] a) D. F. Bainton, *J. Cell Biol.* **1981**, *91*, 66s–76s; b) K. Okamoto, *J. Cell Biol.* **2014**, *205*, 435–445.
[5] a) V. I. Korolchuk, S. Saiki, M. Lichtenberg, F. H. Siddiqi, E. A. Roberts, S. Imarisio, L. Jahreiss, S. Sarkar, M. Futter, F. M. Menzies, C. J. O'Kane, V. Deretic, D. C. Rubinsztein, *Nat. Cell Biol.* **2011**, *13*, 453–460; b) T. Kirkegaard, M. Jäättelä, *Biochim. Biophys. Acta, Mol. Cell Res.* **2009**, *1793*, 746–754.
[6] a) Q. Wan, S. Chen, W. Shi, L. Li, H. Ma, *Angew. Chem.* **2014**, *126*, 11096–11100; b) X. F. Zhang, T. Zhang, S. L. Shen, J. Y. Miao, B. X. Zhao, *J. Mater. Chem. B* **2015**, *3*, 3260–3266; c) W. J. Wang, P. Ning, Q. Wang, W. Zhang, J. Jiang, Y. Feng, X. M. Meng, *J. Mater. Chem. B* **2018**, *6*, 1764–1770.
[7] N. B. Finter, *J. Gen. Virol.* **1969**, *5*, 419–427.
[8] A. C. Allison, M. R. Young, *Lysosomes in biology and pathology*, Elsevier, Amsterdam, Vol. 2, pp. 600–628.
[9] a) C. Svendsen, D. J. Spurgeon, P. K. Hankard, *Ecotoxicol. Environ. Saf.* **2004**, *57*, 20–29; b) A. Pierzyńska-Mach, P. A. Janowski, J. W. Dobrucki, *Cytometry Part A* **2014**, *85*, 729–737.
[10] Z. Li, Y. Song, Y. Yang, L. Yang, X. Huang, J. Han, S. Han, *Chem. Sci.* **2012**, *3*, 2941–2948.

[11] a) J. C. Jiang, X. H. Tian, C. Z. Xu, S. X. Wang, Y. Feng, M. Chen, H. Z. Yu, M. Z. zhu, X. M. Meng, *Chem. Commun.* **2017**, *53*, 3645 – 3648; b) L. L. Hou, P. Ning, Y. Feng, Y. Q. Ding, L. Bai, L. Li, H. Z. Yu, X. M. Meng, *Anal. Chem.* **2018**, *90*, 7122 – 7126.

[12] a) J. Luo, Z. Xie, J. W. Y. Lam, L. Cheng, H. Chen, C. Qiu, H. S. Kwok, X. Zhan, Y. Liu, D. Zhu, B. Z. Tang, *Chem. Commun.* **2001**, 1740 – 1741; b) Y. Hong, J. W. Y. Lam, B. Z. Tang, *Chem. Soc. Rev.* **2011**, *40*, 5361 – 5388; c) J. Mei, Y. Hong, J. W. Y. Lam, A. Qin, Y. Tang, B. Z. Tang, *Adv. Mater.* **2014**, *26*, 5429 – 5479; d) J. Mei, N. L. C. Leung, R. T. K. Kwok, J. Y. W. Lam, B. Z. Tang, *Chem. Rev.* **2015**, *115*, 11718 – 11940.

[13] a) W. Qin, P. Zhang, H. Li, J. W. Y. Lam, Y. Cai, R. T. K. Kwok, J. Qian, W. Zheng, B. Z. Tang, *Chem. Sci.* **2018**, *9*, 2705 – 2710; b) M. T. Gabr, F. C. Pigge, *Dalton Trans.* **2018**, *47*, 2079 – 2085.

[14] a) W. Chen, C. Gao, X. Liu, F. Liu, F. Wang, L. J. Tang, J. H. Jiang, *anal. Chem.* **2018**, *90*, 8736 – 8741; b) M. Grossi, M. Morgunova, S. Cheung, D. Scholz, E. Conroy, M. Terrile, A. Panarella, J. C. Simpson, W. M. Gallagher, D. F. O'Shea, *Nat. Commun.* **2016**, *7*, 10855 – 10868; c) W. C. Zhu, X. J. Zheng, Y. Huang, Z. Y. Lu, H. Ai, *Sci. China Chem.* **2018**, *61*, 483 – 489; d) Y. B. Zhou, H. X. Liu, N. Zhao, Z. M. Wang, M. Z. Michael, N. Xie, B. Z. Tang, Y. H. Tang, *Sci. China Chem.* **2018**, *61*, 892 – 897; e) K. P. Prasad, A. Than, N. Li, M. A. SK, H. W. Duan, K. Y. Pu, X. T. Zheng, P. Chen, *Mater. Chem. Front.* **2017**, *1*, 152 – 157; f) C. W. T. Leung, Z. M. Wang, E. G. Zhao, Y. N. Hong, S. J. Chen, R. T. K. Kwok, A. C. S. Leung, R. We, B. S. Li, J. W. Y. Lam, B. Z. Tang, *Adv. Healthcare Mater.* **2016**, *5*, 427 – 431; g) M. Gao, Q. L. Hu, G. X. Feng, B. Z. Tang, B. Liu, *J. Mater. Chem. B* **2014**, *2*, 3438 – 3442; h) F. Hu, B. Liu, *Org. Biomol. Chem.* **2016**, *14*, 9931 – 9944.

[15] Z. Wang, C. Gui, E. Zhao, J. Wang, X. Li, A. Qin, Z. Zhao, Z. Yu, B. Tang, *ACS Appl. Mater. Interfaces* **2016**, *8*, 10193 – 10200.

[16] S. Wullschleger, R. Loewith, M. N. Hall, *Cell* **2006**, *124*, 471 – 484.

[17] E. F. C. Blommaart, J. J. F. P. Luiken, P. J. E. Blommaart, G. M. van Woerkom, A. J. Meijer, *J. Biol. Chem.* **1995**, *270*, 2320 – 2326.

[18] P. O. Seglen, P. B. Gordon, *Proc. Natl. Acad. Sci. USA* **1982**, *79*, 1889 – 1892.

[19] J. Hardy, D. J. Selkoe, *Science* **2002**, *297*, 353 – 356.

Manuscript received: November 14, 2018
Revised manuscript received: December 20, 2018
Accepted manuscript online: January 2, 2019
Version of record online: January 11, 2019